The Analysis of a Two-Phase Zone with Condensation in a Porous Medium

L. Bridge[1], R. Bradean [2], M. J. Ward [3], B. R. Wetton [4]

Abstract

The one-dimensional steady-state heat and mass transfer in a two-phase zone of a water-saturated porous medium is studied. The system consists of a sand-water-vapour mixture in a tube that is heated from above and cooled from below. Under certain conditions, a two-phase zone of both vapour and water exists in the middle of the tube. A model problem for the temperature and the liquid saturation profiles within this two-phase zone is formulated by allowing for an explicit temperature dependence for the saturation vapour pressure together with an explicit saturation dependence for the capillary pressure. A boundary layer analysis is performed on this model in the asymptotic limit of a large vapour pressure gradient. This asymptotic limit is similar to the large activation energy limit commonly used in combustion problems. In this limit, and in the outer region away from any boundary layers, it is shown that the temperature profile is slowly varying and that the corresponding saturation profile agrees very well with that obtained in the previous model of Udell [Journ. Heat Transfer, **105**, (1983), p. 485] where strict isothermal conditions were assumed. The condensation and evaporation occurring within the boundary layers near the edges of the two-phase zone is examined. Finally, an iterative method is described that allows the temperature profile in the two-phase zone to be coupled to the temperature profiles in the two single-phase zones consisting of either water or vapour. This allows for the computation of the locations of the edges of the two-phase zone within the tube. Numerical computations are performed with realistic values of the parameters.

Keywords: condensation, boundary layer, porous pack

1 Introduction

An understanding of heat transfer and fluid flow through porous media is central for analyzing many environmental and technological applications. Soil is one of many geological materials that is both porous and permeable for the liquids and gases with which it naturally interacts. Waste disposal often requires fluid transport through a porous structure, as does oil recovery, where thermal effects are also significant. The design of porous insulation clearly raises issues of heat transfer and the migration of moisture. The modelling of these and other such processes must take into account the geometry of the porous solid, which impedes the flow of the fluid through the medium.

[1]Department of Mathematics, University of British Columbia, Vancouver, Canada V6T 1Z2
[2]Ballard Power Systems Inc., Burnaby B.C., Canada
[3]Department of Mathematics, University of British Columbia, Vancouver, Canada V6T 1Z2 (corresponding author)
[4]Department of Mathematics, University of British Columbia, Vancouver, Canada V6T 1Z2

The problem of modelling heat and mass transfer of a single-phase fluid flowing through a porous medium is somewhat challenging. A significantly more complicated modeling problem concerns the motion of a fluid through a porous structure that undergoes a phase change. An example of such a problem includes the drying of wood (cf. Whitaker [1]). Fluid phase change in porous media is also at the centre of many technological problems. In configurations involving condensation and evaporation, regions of single-phase fluid and two-phase fluid often coexist within the porous medium.

One technological advance inspired by environmental concerns is the development of the proton exchange membrane (PEM) fuel cell. In recent years, as automotive manufacturers have recognized the need for a low-emission alternative to the internal combustion engine, the design of fuel cells has attracted much interest. This technological advance has required an understanding of the behavior of mathematical models for the condensation of water vapour inside a porous electrode. Bradean *et al.* [2] identifies regions of water vapour oversaturation within a fuel cell electrode, where condensation is likely to occur. Phase change effects are not considered in his model. In this paper, we present a one-dimensional, steady-state model of heat and mass transfer in a porous layer, including phase change effects. Our aim is to form an understanding of this phase-change problem by developing solution techniques that may, hopefully, be extended subsequently to a two-dimensional model of a porous electrode.

A one-dimensional study by Udell [3] investigates the effects on a porous layer, which contains water, of heating the layer at the top and cooling the layer from below. Experimental results indicate that, at steady state, there are three distinct zones within the porous pack: a vapour zone at the top, a liquid zone at the bottom, and a two-phase zone in between. In the two-phase zone there is a counterflow of liquid, driven upwards by capillary forces, and vapour, driven downwards by a pressure gradient. Udell presents a model of the two-phase zone that assumes a constant temperature throughout this zone, with condensation and evaporation occurring at the lower and upper boundaries, respectively. The model problem is solved to give a saturation profile, which indicates the length of the two phase zone. A similar study is performed by Torrance [4], with heating from the bottom, and similar results are obtained.

In this paper, we present an extension to existing models of the two-phase zone. By adding an energy equation to the system considered by Udell [3], and assuming an explicit temperature dependence for the vapour pressure, we are able to solve not only for the saturation, but also for the temperature. In identifying a boundary layer near the lower boundary of the two-phase zone, we are able to show that Udell's formulation is an approximation to the full problem in the large vapour pressure gradient limit. Further, the inclusion of temperature in our model allows us to compute the position of the two-phase zone, as well as the length of it. By coupling the boundary conditions for the two-phase zone to the simple saturation and temperature profiles in the two single-phase zones, we formulate a problem based on the continuity of temperature throughout all three zones, and obtain continuous

saturation and temperature over the entire domain.

The outline of this paper is as follows. In Section 2 we formulate a system of differential equations for the saturation and the temperature profiles within the two-phase zone. In Section 3 we introduce a non-dimensionalization of this system. In doing so, we identify a large parameter based on a large vapour pressure gradient, and we construct an approximate boundary layer solution to this system. The analysis is similar in spirit to the well-known large activation energy limit in combustion theory (cf. [5, pp. 76–84], [6]). In Section 4 we compare the asymptotic theory with numerical solutions to the full coupled problem within the two-phase zone. Finally, in Section 5 we formulate an iterative algorithm to couple the temperature profiles within the vapour-only and water-only one-phase zones at the top and bottom of the porous pack, respectively, to the temperature profile in the middle two-phase zone. Numerical realizations of this algorithm are presented. Finally, some conclusions are made in Section 6.

2 Modelling the Two-Phase Zone

Here we develop a one-dimensional model for steady-state heat and mass transfer within the two-phase zone of a porous layer, heated from the top, cooled from the bottom, and containing a specified mass of water. The configuration is shown in Figure 1 (a).

Suppose that the heat flux through the porous pack maintains three distinct zones as shown in Figure 1 (a). At the top, there is a zone containing only water vapour. In this top zone, phase change does not occur, and heat transfer is through conduction only. Similarly, at the bottom, there is a conductive zone of only liquid water. In between, there is a zone where both liquid and vapour occur. In this middle zone, the liquid is driven upwards through the pores of the porous medium by capillary forces, and the vapour flows countercurrent to the liquid, driven by a pressure gradient. Phase change in our model is assumed to be possible anywhere in this two-phase zone. One of our aims is to find the length, L, of this zone. We model the heat and mass transfer with phase change effects, following the approaches as described in Bridge [12, Chapter 2] and Whitaker [1].

At steady-state, mass conservation may be written as

$$\frac{d}{dz}(\rho_l u_l + \rho_v u_v) = 0\,, \tag{2.1}$$

where u is velocity, ρ is density, and the subscripts l and v refer to the liquid and vapour phases, respectively. Since the fluid in each of the two conductive zones must be stationary, there must be zero mass flux across the boundaries of the two-phase zone. Hence, (2.1) can be integrated to give the overall mass balance

$$\rho_l u_l + \rho_v u_v = 0\,. \tag{2.2}$$

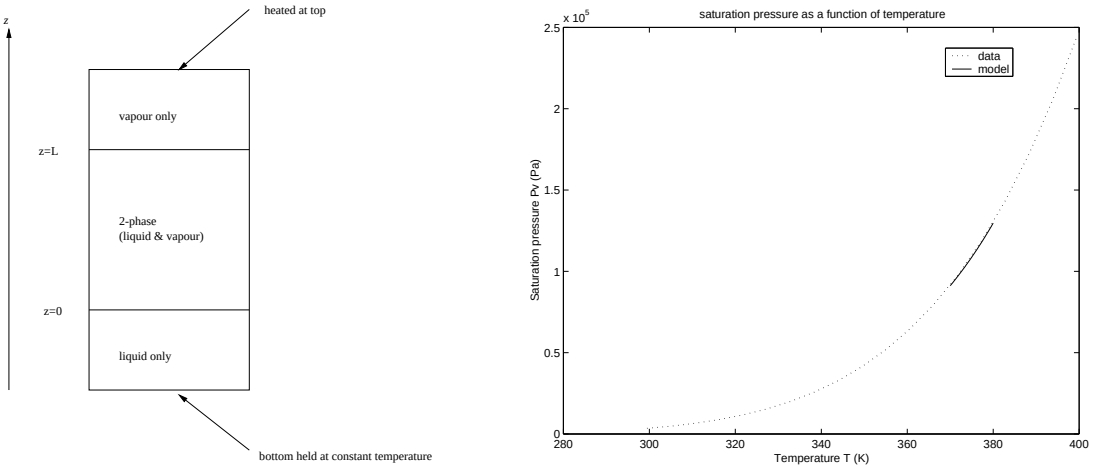

(a) (b)

Figure 1: (a) The three distinct zones. (b) The exponential fit of the saturation pressure with the data of [9].

The local rate of condensation, Γ, is defined by

$$-\Gamma = \frac{d}{dz}(\rho_v u_v)\,. \tag{2.3}$$

Darcy's law gives relations between the velocity and the pressure gradient for each of the two phases as follows (cf. [3]):

$$u_l = \frac{-\kappa\kappa_{rl}}{\mu_l}\left(\frac{dp_l}{dz} + \rho_l g\right)\,, \tag{2.4}$$

$$u_v = \frac{-\kappa\kappa_{rv}}{\mu_v}\left(\frac{dp_v}{dz} + \rho_v g\right)\,. \tag{2.5}$$

Here, κ is the permeability of the porous material, κ_r denotes the relative permeability of a particular phase, μ is the dynamic viscosity, p is the pressure, and g is the acceleration due to gravity.

The energy equation describing the heat transfer and phase change in the two-phase zone is

$$(\rho_l c_l u_l + \rho_v c_v u_v)\frac{dT}{dz} = \frac{d}{dz}\left(\hat{K}\frac{dT}{dz}\right) + h_{vap}\Gamma\,. \tag{2.6}$$

Here, c denotes the specific heat capacity of a particular phase, h_{vap} is the specific latent heat of water, $\hat{K}$ is the thermal conductivity and T is the temperature, which is the same for both phases at any given z. Substituting for u_l and u_v in (2.1), and using (2.4) and (2.5),

we obtain

$$\frac{d}{dz}\left[\frac{\rho_l}{\mu_l}\kappa_{rl}\left(\frac{dp_l}{dz}+\rho_l g\right)+\frac{\rho_v}{\mu_v}\kappa_{rv}\left(\frac{dp_v}{dz}+\rho_v g\right)\right]=0\,. \tag{2.7}$$

The mass balance (2.2) gives the liquid velocity in terms of the vapour velocity, and hence we may write the energy equation (2.6) as

$$(c_v-c_l)\rho_v u_v\frac{dT}{dz}=\frac{d}{dz}\left(\hat{K}\frac{dT}{dz}\right)+h_{vap}\Gamma\,.$$

Using (2.3) and (2.5) to write Γ and u_v in terms of the vapour pressure, p_v, we can write the equation above as

$$\frac{\kappa\rho_v(c_l-c_v)\kappa_{rv}}{\mu_v}\left(\frac{dp_v}{dz}+\rho_v g\right)\frac{dT}{dz}=\frac{d}{dz}\left[\hat{K}\frac{dT}{dz}+\frac{\kappa\rho_v h_{vap}}{\mu_v}\kappa_{rv}\left(\frac{dp_v}{dz}+\rho_v g\right)\right]\,. \tag{2.8}$$

Equations (2.8) and (2.7) form a coupled system of two equations for the variables p_l, p_v, κ_{rl}, κ_{rv} and T. We now make use of some empirical and analytical results to reduce the number of variables in this system.

Firstly, from Baggio *et al.* [8], the vapour pressure in a porous medium may be written as

$$p_v=p_{sat}\exp\left[\frac{-p_c M}{\rho_l R T}\right]\,, \tag{2.9}$$

where p_{sat} is the saturation vapour pressure, M the molar mass of water, and R the universal gas constant. From the data given in [8], the exponent in (2.9) has a typical magnitude 10^{-5}, and we shall hence take $p_v=p_{sat}$ in the analysis that follows. The saturation vapour pressure, p_{sat}, does depend on temperature. The relationship is tabulated in [9]. This data suggests an exponential-type relationship of the form

$$p_v=p_{sat}=ae^{bT}\,,$$

for some constants a and b. Fitting the data in [9] to this curve for temperatures close to 370 K, which are relevant to our model, we obtain the dimensional quantities

$$a=0.19743\text{ Pa}\qquad\text{and}\qquad b=0.03525\text{ K}^{-1}\,. \tag{2.10}$$

In Figure 1 (b) we compare our exponential fit of the data with the data of [9].

Secondly, the capillary pressure, p_c, is defined as the difference between the vapour and liquid pressures,

$$p_c=p_v-p_l\,. \tag{2.11}$$

As shown by Leverett [10], the capillary pressure is found to be a function of the liquid volume fraction, called the saturation s. The functional form for the capillary pressure,

$p_c = p_c(s)$ is known as the Leverett function. Udell [3] correlates this Leverett function to write the capillary pressure as

$$\begin{aligned} p_c &= \delta J(s) \\ &= \delta \left[1.417(1-s) - 2.120(1-s)^2 + 1.263(1-s)^3\right] . \end{aligned} \tag{2.12}$$

Here,

$$\delta = \sigma \left(\frac{\epsilon}{\kappa}\right)^{\frac{1}{2}} ,$$

where σ is the vapour-liquid interfacial tension, and ϵ is the porosity of the porous medium.

Finally, the relative permeabilities are functions of the saturation. The relative permeabilities account for the decrease in mobility of one phase due to the presence of another. Thus, we expect κ_{rl} to be zero when only liquid is present, and unity for only vapour. Similarly, κ_{rv} should be zero when $s = 1$ and unity when $s = 0$. We will use the cubic forms suggested by Udell [3] to represent the results reported by Fatt and Klickoff [11].

In summary, we have the following empirical relationships:

$$\kappa_{rl} = s^3 , \tag{2.13}$$

$$\kappa_{rv} = (1-s)^3 , \tag{2.14}$$

$$p_v = ae^{bT} , \tag{2.15}$$

$$p_l = ae^{bT} - \delta J(s) . \tag{2.16}$$

Substituting (2.13)-(2.16) into equations (2.7) and (2.8), we obtain two coupled equations for s and T

$$\frac{d}{dz}\left[\frac{\rho_l}{\mu_l}s^3\left(\frac{d}{dz}[ae^{bT} - \delta J(s)] + \rho_l g\right) + \frac{\rho_v}{\mu_v}(1-s)^3\left(\frac{d}{dz}[ae^{bT}] + \rho_v g\right)\right] = 0 , \tag{2.17}$$

and

$$\begin{aligned} &\frac{\kappa\rho_v(c_l - c_v)}{\mu_v}(1-s)^3\left(\frac{d}{dz}[ae^{bT}] + \rho_v g\right)\frac{dT}{dz} \\ &= \frac{d}{dz}\left[\hat{K}\frac{dT}{dz} + \frac{\kappa\rho_v h_{vap}}{\mu_v}(1-s)^3\left(\frac{d}{dz}[ae^{bT}] + \rho_v g\right)\right] . \end{aligned} \tag{2.18}$$

2.1 Boundary Conditions

The system (2.17), (2.18) is second order in both s and T, and thus requires four boundary conditions. At the top of the two-phase zone, representing the boundary with the vapour-only zone, the saturation is zero. The heat flux across the boundary, q, which we will initially

specify, accounts for the temperature gradient and the evaporation of the upwards flowing liquid water at the boundary. Thus, the two conditions at the upper boundary are

$$\hat{K}\frac{dT}{dz} = q - h_{vap}\rho_l u_l\,, \qquad s = 0\,, \qquad \text{at } z = L\,. \tag{2.19}$$

Since we are considering a one-dimensional problem with no radial heat losses, the heat flux across the lower boundary must also be q. Here, the associated phase change is condensation of the downward flowing vapour, and the saturation is unity. Thus, the conditions at the lower boundary are

$$\hat{K}\frac{dT}{dz} = q + h_{vap}\rho_v u_v, \qquad s = 1\,, \qquad \text{at } z = 0\,. \tag{2.20}$$

The coupled system for $s = s(z)$ and $T = T(z)$ is given by the second order equations (2.17) and (2.18), subject to the boundary conditions (2.19) and (2.20). In this system the length L of the two-phase zone is unknown. Thus, we must specify the temperature at one of the edges of the two-phase zone. This is done below following (3.5).

2.2 Nondimensionalization

We now nondimensionalize the system using the following scalings:

$$z = \frac{\delta}{\rho_l g}z^*\,, \qquad L = \frac{\delta}{\rho_l g}L^*\,, \qquad p_c = \delta p_c^* \quad \text{with} \quad \delta = \sigma\left(\frac{\epsilon}{\kappa}\right)^{\frac{1}{2}}\,,$$

$$T = T_{ref}T^*, \qquad \hat{K} = \hat{K}_l\hat{K}^*, \qquad q = \frac{\kappa h_{vap}\rho_v\rho_l g}{\mu_l}q^*\,.$$

Here * denotes a dimensionless quantity. In terms of these variables, (2.17) becomes

$$\frac{d}{dz^*}\left[s^3\left(\frac{d}{dz^*}\left[\frac{a}{\delta}e^{bT_{ref}T^*} - J(s)\right] + 1\right) + \alpha\beta(1-s)^3\left(\frac{d}{dz^*}\left[\frac{a}{\delta}e^{bT_{ref}T^*}\right] + \alpha\right)\right] = 0\,. \tag{2.21}$$

Similarly, (2.18) transforms to

$$\begin{aligned}&\frac{\kappa\rho_v(c_l - c_v)}{\mu_v}(1-s)^3\left(\frac{a}{\delta}\frac{d}{dz^*}\left[e^{bT_{ref}T^*}\right] + \alpha\right)T_{ref}\frac{dT^*}{dz^*}\\ &= \frac{d}{dz^*}\left[\hat{K}_l\hat{K}^*\frac{T_{ref}}{\delta}\frac{dT^*}{dz^*} + \frac{\kappa\rho_v h_{vap}}{\mu_v}(1-s)^3\left(\frac{a}{\delta}\frac{d}{dz^*}\left[e^{bT_{ref}T^*}\right] + \alpha\right)\right]\quad .\end{aligned} \tag{2.22}$$

Here we have defined $\alpha = \rho_v/\rho_l$ and $\beta = \mu_l/\mu_v$. The Rayleigh number Ra for this problem is given by

$$Ra = \frac{\kappa\rho_v(c_l - c_v)\delta}{\mu_l\hat{K}_l}\,. \tag{2.23}$$

In Table 1 we list typical values for dimensional and dimensionless quantities of interest using the data given in Udell [3] and Bridge [12, Chapter 2]. This allows us to identify the orders of magnitude associated with certain parameters in our model.

From the data given in Table 1, we see that $Ra = \mathcal{O}(10^{-1})$, while terms on the right-hand side of equation (2.22) are on the order of 10^2. Thus, the two-phase zone corresponds to a small Rayleigh number problem. That is, diffusive effects are dominant over convective effects. Thus, we neglect the left-hand side of the energy equation (2.22). The right hand side of (2.22) can then be integrated, giving

$$\hat{K}_l \hat{K}^* \frac{T_{ref}}{\delta} \frac{dT^*}{dz^*} + \frac{\kappa \rho_v h_{vap}}{\mu_v} (1-s)^3 \left(\frac{a}{\delta} \frac{d}{dz^*} \left[e^{bT_{ref} T^*} \right] + \alpha \right) = C \,, \tag{2.24}$$

where C is a constant to be determined. For the subsequent analysis, we choose $T_{ref} = 380\text{K}$, to ensure that $T^* \approx 1$.

3 Asymptotic Analysis

We now formulate our problem as concisely as possible. Multiplying the energy equation (2.24) by $\delta / \hat{K}_l T_{ref}$, we obtain

$$\hat{K}^* \frac{dT^*}{dz^*} + \eta (1-s)^3 \left(\frac{a}{\delta} \frac{d}{dz^*} \left[e^{bT_{ref} T^*} \right] + \alpha \right) = \hat{C} \,, \tag{3.1}$$

where η is defined by

$$\eta = \frac{\kappa \rho_v h_{vap} \delta}{\mu_v \hat{K}_l T_{ref}} \,.$$

Again, the constant $\hat{C}$ is to be determined. We notice that (3.1) is simply a nondimensional version of

$$\hat{K} \frac{dT}{dz} + h_{vap} \rho_v u_v = \text{constant}. \tag{3.2}$$

The boundary condition (2.20) shows that the constant in (3.2) is the heat flux, q. In view of the overall mass balance, we note that the condition (2.19) is then automatically satisfied by (3.2). Thus, upon neglecting the convective term in the energy equation that is proportional to the Rayleigh number, a heat flux boundary condition at the bottom of the two-phase zone is automatically satisfied once the heat flux boundary condition at the top of the two-phase zone is satisfied. In addition, the constant $\hat{C}$ in (3.1) is a scaled heat flux defined by

$$\hat{C} = \frac{\delta}{\hat{K}_l T_{ref} \rho_l g} q \,. \tag{3.3}$$

Table 1: List of parameters and variables used.

Symbol	Interpretation	Typical value	Units (SI)
Dimensional parameters			
κ	permeability	6.4×10^{-12}	m^2
ρ_v	vapor density	1	kg/m^3
ρ_ℓ	liquid density	10^3	kg/m^3
c_v	specific heat of vapor	10^3	$J/kg\,K$
c_ℓ	specific heat of liquid water	$4.1 - 4.3 \times 10^3$	$J/kg\,K$
μ_v	viscosity of water vapour	2.2×10^{-5}	$kg/m\,s$
μ_ℓ	viscosity of liquid water	2.5×10^{-4}	$kg/m\,s$
$\hat{K}_v$	thermal conductivity of vapor saturated porous medium	1.0	$W/m\,K$
$\hat{K}_l$	thermal conductivity of liquid saturated porous medium	2.5	$W/m\,K$
q	heat flux	10^3	W/m^2
h_{vap}	latent heat (water liquid-vapor)	2.5×10^6	J/kg
σ	surface tension (water liquid-vapor)	72.4×10^{-3}	kg/s
R	universal gas constant	8.31	$J/mole\,K$
M	molar mass of water	18×10^{-3}	$kg/mole$
g	acceleration due to gravity	9.8	m/s^2
a	characteristic vapour pressure - see (2.10)	0.19743	Pa
b	characteristic temperature scaling - see (2.10)	0.03525	K^{-1}
H	total height of porous pack	0.254	m
T_{ref}	reference temperature	380	K
Dimensional variables			
T	temperature	$360 - 390$	K
p_v	vapor pressure	$0.7 - 1.4 \times 10^5$	Pa
p_c	capillary pressure	$0 - 1 \times 10^4$	Pa
Non-dimensional parameters			
ϵ	porosity	0.38	—
α	density ratio (ρ_v/ρ_ℓ)	10^{-3}	—
β	viscosity ratio (μ_ℓ/μ_v)	11	—
ϕ	see (3.6)	13.4	—
η	see (3.1)	13.5	—
ξ	see (3.9)	13.5	—
D	total height of porous pack	0.14	—
Non-dimensional variables			
s	liquid volume fraction	$0 - 1$	—
T	temperature	$0.95 - 1.05$	—
p_v	vapor pressure	$3.98 - 8.13$	—
p_c	capillary pressure	$0 - 0.6$	—

Sources: Bradean in [12], Udell [3].

The problem now is reduced to solving the first order system

$$s^3\left(\frac{d}{dz^*}\left[\frac{a}{\delta}e^{bT_{ref}T^*}-J(s)\right]+1\right)+\alpha\beta(1-s)^3\left(\frac{d}{dz^*}\left[\frac{a}{\delta}e^{bT_{ref}T^*}\right]+\alpha\right)=0, \tag{3.4}$$

$$\hat{K}^*\frac{dT^*}{dz^*}+\eta(1-s)^3\left(\frac{a}{\delta}\frac{d}{dz^*}\left[e^{bT_{ref}T^*}\right]+\alpha\right)=\hat{C}\,, \tag{3.5}$$

subject to the conditions $s(0)=1$, $s(L^*)=0$ for the unknown nondimensional two-phase zone length L^*, with T^* specified at one of the boundaries. We need to specify this extra condition on T^* since the trivially satisfied heat flux condition leaves us with insufficient data to solve the system. In practice, in §5 we will later determine T^* at the boundaries of the two-phase zone in terms of the temperatures at the bottom and top of the entire porous pack. This will be done by coupling the temperature profiles in all three distinct zones together such that the temperature is continuous throughout the entire porous pack.

The analysis of the system is assisted by the identification of the large parameter ϕ defined by

$$\phi=bT_{ref}\,. \tag{3.6}$$

We use the value of b from (2.10) and the value $T_{ref}=380\text{K}$ to calculate that $\phi\approx 13.4$. Since our choice of T_{ref} ensures that $T^*=\mathcal{O}(1)$, we have that $e^{bT_{ref}T^*}=e^{\phi T^*}$ is large. This implies that we have an exponentially large vapour pressure, and an exponentially large vapour pressure gradient throughout the two-phase zone.

Exponential nonlinearities that can range over many orders of magnitude are common in combustion problems where reactions are controlled by Arrhenius reaction rates that depend exponentially on the temperature. An asymptotic method to treat these problems was introduced in [5, pp. 76–84]. This method is now commonly referred to as high activation energy asymptotics (cf. [7, Chapter 2]). High activation energy asymptotics is in fact one of a variety of asymptotic methods used to treat problems where either exponentially large or exponentially small effects need to be resolved. Here, for our condensation problem, we use a similar approach to the large activation energy asymptotic method used by Kapila and Matkowsky [6]. Factorizing the exponential term in (3.5) as $e^{\phi}e^{\phi(T^*-1)}$, we can write the system (3.4) and (3.5) as

$$s^3\left(\xi\frac{d}{dz^*}\left[e^{\phi(T^*-1)}\right]-\frac{d}{dz^*}J(s)+1\right)+\alpha\beta(1-s)^3\left(\xi\frac{d}{dz^*}\left[e^{\phi(T^*-1)}\right]+\alpha\right)=0, \tag{3.7}$$

$$\underbrace{\hat{K}^*}_{\sim 1}\frac{dT^*}{dz^*}+\eta(1-s)^3\left(\xi\frac{d}{dz^*}\underbrace{\left[e^{\phi(T^*-1)}\right]}_{\mathcal{O}(1)}+\alpha\right)=\hat{C}, \tag{3.8}$$

where

$$\xi = \frac{a}{\delta} e^{\phi}. \tag{3.9}$$

We refer to (3.7) and (3.8) as the full problem. In the discussion below we drop the * in this system.

The data in Table 1 gives $\xi \approx 7.3$, $\eta \approx 13.5$, and $\hat{K} = \mathcal{O}(1)$. Since $\phi \approx 13.4$, we will solve this system in the following asymptotic limit:

$$\xi = \mathcal{O}(1) \ \text{ and } \ \eta = \mathcal{O}(\phi)\,. \tag{3.10}$$

Before analyzing the asymptotic structure of (3.7) and (3.8), we determine the asymptotic behavior of the saturation s and the temperature T near the boundaries of the two-phase zone. Using the method of dominant balance, we readily obtain near the top boundary at $z = L$ that (see [12, Chapter 3])

$$s \sim B(L - z)^{1/4}\,, \qquad z \to L\,, \tag{3.11}$$

and

$$T \sim T_{top} - E(L - z)\,, \qquad z \to L\,, \tag{3.12}$$

where the constants B and E are given by

$$E = \frac{\hat{C} - \eta\alpha}{\hat{K} + \eta\xi\phi e^{\phi(T_{top}-1)}}\,, \tag{3.13}$$

and

$$B = \left(\frac{-4\alpha\beta(\hat{C} - \hat{K}E)}{J'(0)\eta} \right)^{1/4}. \tag{3.14}$$

Here T_{top} is the value of T at $z = L$. From (3.11) it follows that $s'(z)$ is singular at $z = L$. This singularity has the potential for being troublesome when computing numerical solutions. In §4 we discuss a regularized model amenable to finite difference computations.

Now, denoting the temperature at the lower boundary of the two-phase zone by T_{bot}, a dominant balance analysis yields the asymptotic forms

$$s \sim 1 - Fz\,, \qquad z \to 0\,, \tag{3.15}$$

and

$$T \sim T_{bot} + Gz\,, \qquad z \to 0\,. \tag{3.16}$$

Here, the constants F and G are given by

$$G = \frac{\hat{C}}{\hat{K}}, \tag{3.17}$$

and

$$F = \frac{-1 - \xi\phi e^{\phi(T_{bot}-1)}G}{J'(1)}. \tag{3.18}$$

A higher order expansion proceeds in powers of z and shows that s and T are analytic near $z = 0$.

3.1 Boundary Layer Problem Near $z = 0$

We write (3.8), where $\phi \approx 13.4$ is a large parameter, as

$$\underbrace{\underbrace{\hat{K}}_{\sim 1}\frac{dT^*}{dz^*}}_{\text{term 1}} + \underbrace{\eta(1-s)^3\left(\xi\frac{d}{dz}\underbrace{\left[e^{\phi(T-1)}\right]}_{\mathcal{O}(1)} + \alpha\right)}_{\text{term 2}} = \hat{C}. \tag{3.19}$$

In (3.19) term 1 is small compared with term 2, provided that

$$\eta\xi\phi(1-s)^3 \gg \hat{K},$$

which implies,

$$1 - s \gg \left(\frac{\hat{K}}{(\eta\xi\phi)}\right)^{1/3}. \tag{3.20}$$

Since $\xi = \mathcal{O}(1)$ and $\eta = \mathcal{O}(\phi)$, we can write (3.20) as

$$1 - s \gg \phi^{-2/3}. \tag{3.21}$$

The inequality (3.21) holds unless $s \sim 1 - s_1\phi^{-2/3}$, where $s_1 \sim O(1)$. Thus, since $s(0) = 1$, term 1 in equation (3.19) is negligible except in a thin layer near $z = 0$. The width of this boundary layer then clearly tends to zero in the limit $\phi \to \infty$.

In the outer region, away from the lower boundary at $z = 0$, term 1 in (3.19) is negligible, and thus

$$\xi\frac{d}{dz}\left[e^{\phi(T-1)}\right] = \frac{\hat{C}}{\eta(1-s)^3} - \alpha. \tag{3.22}$$

The neglect of the small term uncouples the system (3.7) and (3.8). Substituting (3.22) into (3.7), and rearranging, we obtain

$$s'_{outer}(z) = \frac{(1-\alpha) + \frac{\hat{C}}{\eta}\left[\frac{1}{(1-s)^3} + \frac{\alpha\beta}{s^3}\right]}{J'(s)}. \tag{3.23}$$

The solution to this outer problem for the saturation has a singularity at $s = 0$, in common with the full problem. However, it also has a singularity at $s = 1$. A dominant balance argument gives

$$s \sim \quad 1 - B_1 z^{1/4} \quad \text{as } z \to 0\,, \tag{3.24}$$

$$s \sim \quad B_2 (L - z)^{1/4} \quad \text{as } z \to L\,, \tag{3.25}$$

where

$$B_1 = \sqrt[4]{\frac{-4\hat{C}}{\eta J'(1)}}\,, \tag{3.26}$$

and

$$B_2 = \sqrt[4]{\frac{-4\alpha\beta\hat{C}}{\eta J'(0)}}\,. \tag{3.27}$$

The saturation in the outer region will be found from the numerical solution of (3.23) subject to the outer boundary condition $s(L) = 0$. The outer temperature, which follows from (3.22), is given by

$$T_{outer}(z) = 1 + \frac{1}{\phi} \ln \left[\frac{1}{\xi} \int_L^z \left(\frac{\hat{C}}{\eta (1 - s(t))^3} - \alpha \right) dt + e^{\phi (T_{top} - 1)} \right]\,, \tag{3.28}$$

where the temperature at the upper boundary, T_{top}, must be specified.

We now compare our outer problem with the formulation of Udell [3]. The saturation profile from Udell [3] reduces to solving the first order equation

$$s'(z) = \frac{(1 - \alpha) + \frac{\hat{C}}{\eta} \left[\frac{1}{(1-s)^3} + \frac{\alpha\beta}{s^3} \right]}{(1 - \alpha) J'(s)}\,, \tag{3.29}$$

subject to $s(0) = 1$. Since $\alpha = 0.001$ we have almost perfect agreement with our outer problem (3.23). Therefore, Udell's problem corresponds to our outer solution, and so is not expected to be valid near the lower boundary.

We now consider the physical meaning of the outer solution. In neglecting term 1 in (3.19), we force, in dimensional variables, that $\rho_v u_v h_{vap}$ is a constant. Thus, from (2.3) we get

$$\frac{d}{dz} \left[\rho_v u_v h_{vap} \right] = 0\,, \qquad \Rightarrow \quad \Gamma = 0\,.$$

This implies that the condensation rate is zero everywhere inside the outer region, and thus phase change can only occur at the boundaries. So Udell's model clearly describes an evaporation front at the upper boundary and a condensation front at the lower boundary.

Our boundary layer formulation similarly suggests that evaporation takes place in a front at the upper boundary, with no phase change in the outer region, and that condensation may occur in a layer near the lower boundary. Further insight is gained by writing (3.19) in the form

$$\underbrace{\frac{dT}{dz}}_{\text{term 1}} + \underbrace{\mathcal{O}(\phi)\,(1-s)^3\left(\frac{d\hat{p_v}}{dz}+\hat{\alpha}\right)}_{\text{term 2}} = \hat{C}. \tag{3.30}$$

We see that an $\mathcal{O}(1)$ variation in vapour pressure corresponds to an $\mathcal{O}(1/\phi)$ variation in temperature. The popular isothermal assumption used in the literature (eg. [3], [4]) suggests that diffusive effects are negligible throughout the entire two-phase zone. However, we see that this is only true in the limit $\phi \to \infty$, and we have identified a layer near the lower boundary where diffusion must be considered.

Near the lower boundary, the saturation can be approximated by $s \sim 1$ when $\phi \gg 1$. Thus, inside this layer, (3.7) reduces to

$$\xi \frac{d}{dz}\left[e^{\phi(T-1)}\right] - \frac{d}{dz}J(s) + 1 = 0\,. \tag{3.31}$$

The boundary layer problem for the inner solution is thus given by (3.31) together with (3.19), where term 1 is now retained. The system is then easily decoupled to give

$$\frac{\hat{K}}{\phi}\left(\frac{J'(s)\frac{ds}{dz}-1}{\hat{A}+J(s)-z}\right) + \eta(1-s)^3\left(J'(s)\frac{ds}{dz}-1+\alpha\right) = \hat{C}\,, \tag{3.32}$$

and

$$T = 1 + \frac{1}{\phi}\ln\left[\frac{\hat{A}+J(s)-z}{\xi}\right], \tag{3.33}$$

where the constant $\hat{A}$ is given by

$$\hat{A} = \xi e^{\phi(T_{bot}-1)}\,, \tag{3.34}$$

and T_{bot} is specified.

4 Numerical Solutions

The full coupled problem (3.7) and (3.8) is now solved subject to the condition $s = 1, T = T_{bot}$ at $z = 0$. The temperature T_{bot}, and the heat flux q must be specified, and the length L of the two-phase zone is then found from the upper boundary condition $s(L) = 0$. We employ a 4th/5th order Runge-Kutta scheme, and implement the upper boundary condition as $s(L) = \varepsilon$, where $\varepsilon \ll 1$.

The error made in computing the length L by using this regularized boundary condition is $\mathcal{O}(\varepsilon^4)$ as suggested by (3.25). This error is plotted numerically in [12, Chapter 4]. This shows that computing the outer problem with the boundary conditions $s = \epsilon$ and $s = 1 - \epsilon$ at the ends of the two-phase zone gives high accuracy and involves only nonsingular, well behaved equations that are amenable to computation. Solutions with $T_{bot} = 1$ for various values of the heat flux are shown in Figure 2 (a). As remarked in §3 following (3.29), our saturation profile closely approximates Udell's saturation profile over most of the domain, except in a small region near the lower boundary at $z = 0$. Our computed temperature profiles shown in Figure 2 (a) indicate that the isothermal assumption used by Udell is a good approximation, but is not strictly valid. In particular, there is a sharp increase in the temperature gradient near the lower boundary. However, the change in temperature over the two-phase zone is small, on the order of 0.1%. Thus, in the absence of rather accurate measurements along the entire porous pack, the two-phase zone in Udell's experiment would clearly appear approximately isothermal.

Udell [3] reports that the length of the two-phase zone increases with decreasing heat flux. This qualitative feature is also captured by our model. In particular, our computations show that the two-phase zone length increases from $L \approx 0.06$ when $q = 3200$ to $L \approx 0.14$ when $q = 800$. In Figure 2 (b) we plot the length L as a function of q. This curve enables us to predict the minimum value of the heat flux that is sufficient to support three distict zones for a given overall length of the porous pack. In particular, for Udell's porous pack, which has a nondimensional length of 0.1411, we see that a heat flux of less than a critical value of approximately 600 Wm^{-2} gives $L > 0.1411$, and thus will not support the three distinct zones in a pack of this size together with the given temperature $T_{bot} = 1$.

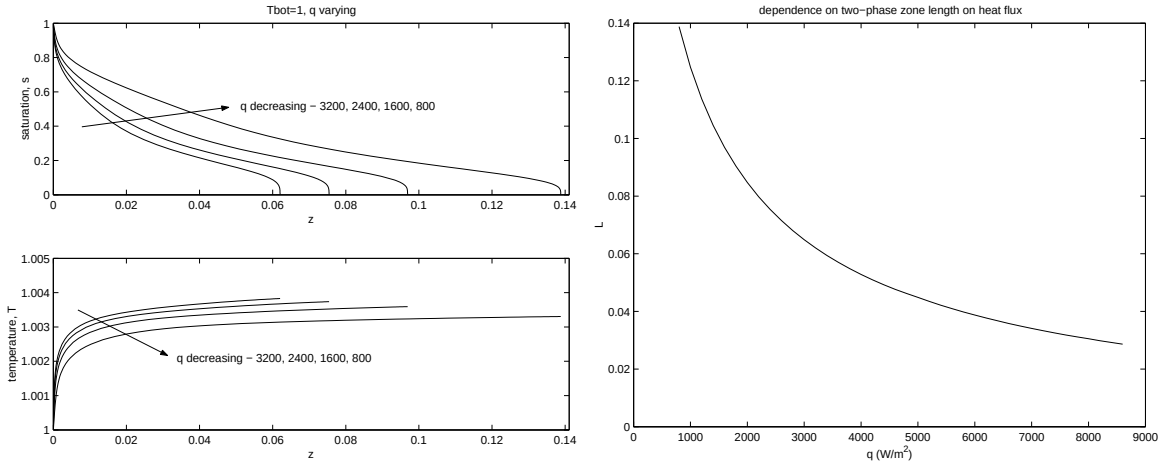

(a) (b)

Figure 2: (a) Numerical solutions to the full problem with different heat flux. (b) Length of the two-phase zone as a function of the applied heat flux.

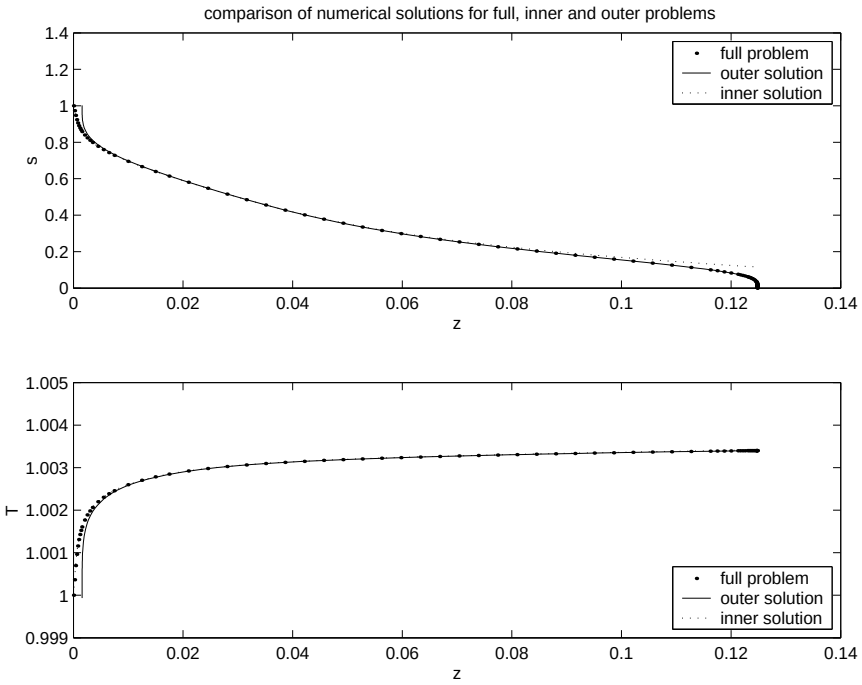

Figure 3: Full and boundary layer solutions.

To find the inner solution, we solve numerically the initial value problem for the saturation given by equations (3.34) and (3.32) with the initial conditions $s(0) = 1$, and T_{bot} specified. This is done using a 4th/5th order Runge-Kutta method. The temperature $T(z)$ is then trivially computed using the algebraic equation (3.33). The outer solution is similarly obtained by solving the saturation problem (3.23) subject to $s(0) = 1$ and $s(L) = 0$, and then applying a numerical quadrature method to compute the temperature given by (3.28). We choose a midpoint method to deal with the improper integral in (3.28) as $s \to 1$. Notice that the length L is unknown in the outer formulation, and for comparison with the full solution, we simply set L to be that which is found from the full solution, and then compute the outer solution.

In Figure 3, we plot the full solution together with the inner and outer solutions for both saturation and temperature. The outer problem is clearly a good approximation to the full problem except for inside the thin boundary layer at the lower boundary.

In the previous section, we showed that the width of the boundary layer tends to zero in the limit $\phi \to \infty$, and thus the outer solution tends to the full solution. In Figure 4 (b), we plot saturation profiles for $\phi = 5,\ 10,\ 13.4$ and 50, computed with $q = 1000$ and $T_{bot} = 1$. We see that the outer solution quickly converges to the full solution as ϕ becomes large. Notice that the saturation profile for our computed value $\phi = 13.4$ is in close agreement with

the profile for $\phi = 50$.

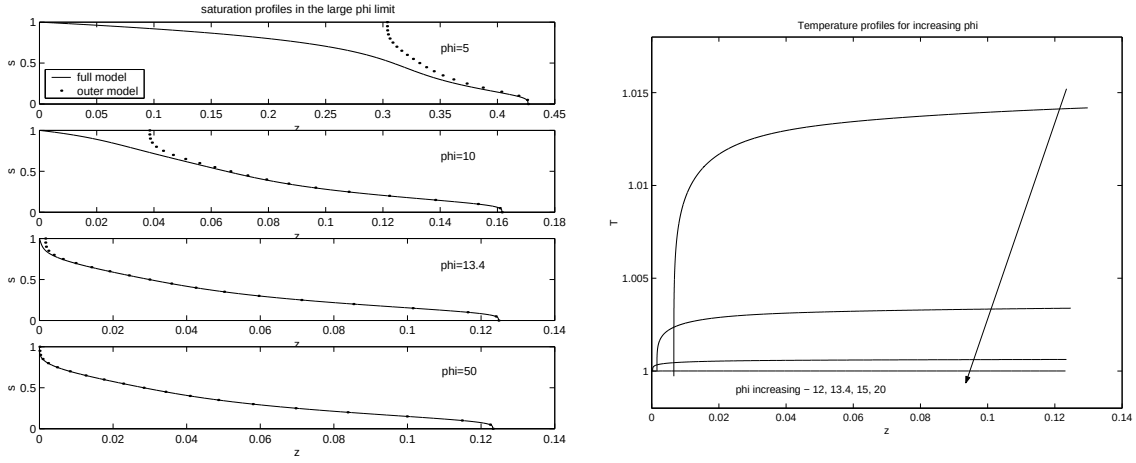

(a) (b)

Figure 4: (a) Full and outer saturation profiles as $\phi \to \infty$. (b) Convergence to constant temperature.

We have also shown that as $\phi \to \infty$, the temperature in the two-phase zone becomes approximately isothermal. In Figure 4 (b), we plot the temperature profiles obtained as ϕ increases through large values. Our computations clearly show the convergence to an approximately isothermal two-phase zone.

5 Coupling to the Single-Phase Zones

Reports on the one-dimensional study of fluid phase change in a heated porous pack have noted the existence of distinct zones containing liquid only, vapour only and both phases. Typically, a model problem is described in the two-phase zone, from which the length of that zone may be found (see [3], [4]). However, the problem of finding the position of the two-phase zone in a three-zone porous pack has so far not been considered. The heat transfer in the two single-phase zones is by conduction only. Thus, the temperature in these zones is harmonic, and has a linear profile. The problem of finding the length of a two-phase zone and its position between the two single-phase zones is formulated from the condition that the temperature is continuous throughout the entire pack.

Consider the one-dimensional porous pack configuration shown in Figure 5 (a). Experimentally, the parameters which we are able to explicitly control are the temperatures applied to the top and bottom of the entire pack. Thus, we consider our temperature control parameters to be T_1 and T_0. Conceivably, we could formulate an inverse problem such that, given the control parameters T_1 and T_0, we can compute the values of the heat flux, q, through

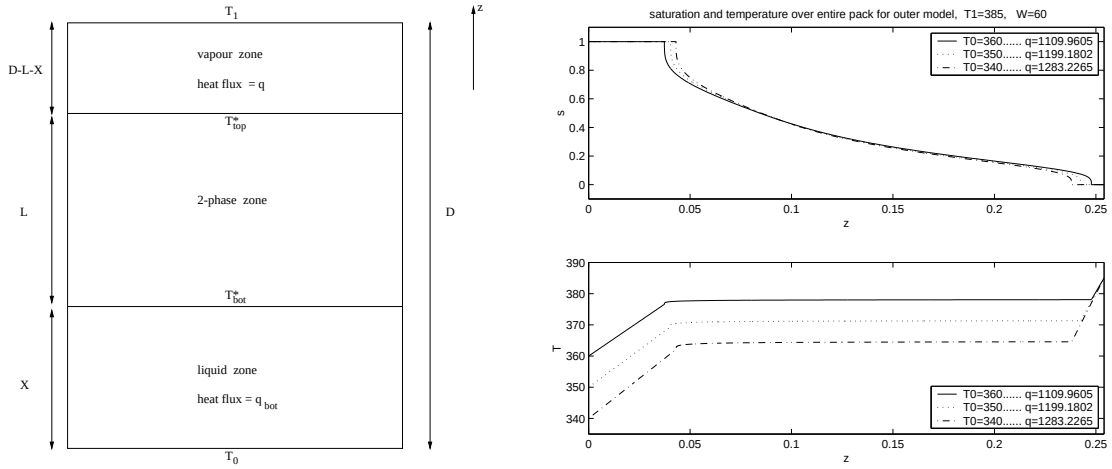

Figure 5: (a) Porous layer and three distinct zones. (b) Profiles for entire pack, with variation in T_0.

the vapour-only zone, and the temperature T_{top} at the top of the two-phase zone. Then the length, $(D - L - X)$, of the vapour zone would be easily computed, since the temperature profile in that zone is linear. Since we would now have q and T_{top} specified, we could compute the values of L and T_{bot} using our solution technique from the previous section. This would determine X is known. However, with T_{bot}, T_0 and X known, and a linear temperature profile in the conductive liquid-only zone, we can calculate the heat flux q_{bot} through this bottom zone. Since we are considering a one-dimensional problem, there is no radial heat loss from the pack. Experimentally, this is achieved by insulating the walls of the container that holds the porous medium. Thus the downward heat flux across the vapour zone must equal the downward heat flux across the liquid zone, and so we have the requirement that

$$q = q_{bot}. \tag{5.1}$$

A further constraint must be incorporated into our model in order to meet this requirement, and so we need a further control parameter for the inverse problem. This third control parameter for the experiment is the total mass of water inside the porous pack. This parameter may obviously be varied for different experiments. The mass in the two conductive zones is trivially computed if their lengths are known, while the mass contained within the two-phase zone will depend on the saturation profile. Suppose the entire pack contains a measured mass (per unit cross sectional area) of water. Then this mass, W, must satisfy the integral constraint

$$X\rho_l + \int_0^L \left(s\rho_l + (1-s)\rho_v\right)\, dz + (D - L - X)\rho_v = W. \tag{5.2}$$

We now pose an inverse problem which, given inputs T_1, T_0 and W, will return all the unknowns shown in Figure 5 (a), and be consistent with the heat flux condition (5.1). In solving this problem, we compute the saturation and temperature profiles within the two-phase zone, and we present the problem for both the outer equations (3.23), (3.28) and the full equations (3.7), (3.8). Further, given the inputs T_1, T_0 and W, the saturation and temperature profiles over the entire porous pack may then be compared for the outer and full models.

For the outer formulation, we have the following equations, valid inside the two-phase zone:

$$s'_{outer}(z) = \frac{(1-\alpha) + \frac{\hat{C}}{\eta}\left[\frac{1}{(1-s)^3} + \frac{\alpha\beta}{s^3}\right]}{J'(s)}, \tag{5.3}$$

and

$$T_{outer}(z) = 1 + \frac{1}{\phi}\ln\left[\frac{1}{\xi}\int_L^z \left(\frac{\hat{C}}{\eta(1-s(t))^3} - \alpha\right) dt + e^{\phi(T_{top}-1)}\right], \tag{5.4}$$

where

$$\hat{C} = \frac{\delta}{\hat{K}_l T_{ref}\rho_l g} q. \tag{5.5}$$

In order to compute for the temperature and the saturation over the entire domain, we iterate according to Algorithm 1, described below.

Algorithm 1

- Input T_1, T_0, W.
- Initialize q.
- Repeat
  - Compute $\hat{C}$ as in (5.5).
  - Solve (5.3) subject to $s(0) = 1$ and $s(L) = 0$. Hence obtain $s(z)$, L.
  - (5.2) gives $X = \frac{W-(D-L)\rho_v - \int_0^L (s\rho_l + (1-s)\rho_v)\, dz}{\rho_l - \rho_v}$.
  - $T_{top} = \left[T_1 - \frac{(D-L-X)*lengthscale}{\hat{K}_v}\, q\right] / T_{ref}$.
  - Compute $T(z)$ according to (5.4). Hence find the temperature T_{bot}.
  - $q_{bot} = \hat{K}_l \frac{T_{bot}*T_{ref} - T_0}{X*lengthscale}$.
  - $f(q) = q - q_{bot}$. (Want $f(q) = 0$ for a solution).
  - Adjust q if necessary by a Newton step.
- Until $\|f(q)\| < tol_q$.

The stopping criterion for this iteration in Algorithm 1 is that $\|q - q_{bot}\| < tol_q$, where tol_q is a user specified tolerance on the heat flux. This criterion ensures that the requirement (5.1) is met to within some tolerance, and setting $tol_q = 1$ gives is sufficient to give a 0.1% difference between q and q_{bot} if q is on the order of 1000 Wm^{-2}.

We implement Algorithm 1 numerically by defining the function $f(q)$ and employing a Newton method to find the roots of f. To solve the outer equations in the two-phase zone we use the numerical techniques and regularization methods described in the previous chapter. The integral in equation (5.2) is computed using Simpson quadrature. Also, for the Newton iterations, we use a centered difference approximation for the derivative $f'(q)$. It is worth noting that for this outer formulation, we are able to find the two parameters q and T_{top} by implementing a single variable root finder. This is due to the fact that the outer problem for $s(z)$ and $T(z)$ may be uncoupled. The inverse problem for the full model, which we will describe in the next section, does not have this convenient property.

Our Newton method implementation of Algorithm 1 is seen to converge to within the specified tolerance, usually in less than 10 iterations. We take our initial value of heat flux q from the data from Udell's experiments [3].

In Figure 5 (b), we plot results for three runs of our code. In each run, we keep the top temperature T_1 and the water content W the same. The three distinct zones within the porous pack are clear from both the saturation and temperature profiles. Also, we can see clearly that the temperature variation over the two-phase zone is very small in comparison with the variations over the two single-phase zones, as expected. By way of validation, as we lower the bottom temperature T_0, we note that the heat flux increases, as expected. With this increase in heat flux, the decrease in the length of the two-phase zone is also apparent.

The results of a further test are shown in Figure 6 (a). Here we hold the temperatures T_1 and T_0 constant. Then the effect of an increase in total water mass W is clearly evident, as the length of the liquid-only zone is seen to increase. Finally, in Figure 6 (b), we choose the three control parameters in such a way that we can demonstrate the effects of large variations in heat flux. Here, we see again the decrease in length of two-phase zone with increasing heat flux, while the increase in liquid-zone length with increasing water mass is again clear.

The iterative inverse problem for the full formulation becomes more complicated, since the full system (3.7), (3.8) cannot be uncoupled. Here, we will initialize the boundary conditions at the lower boundary of the two-phase zone. Thus, we now consider the problem shown in Figure 5 (a), except with the flux in the liquid zone being equal to q. We then follow a similar approach to Algorithm 1, and compute a new heat flux in the vapour-only zone, which we will label q_{top}. We now have an inverse problem for the two parameters q and T_{bot}, which we will solve using Algorithm 2.

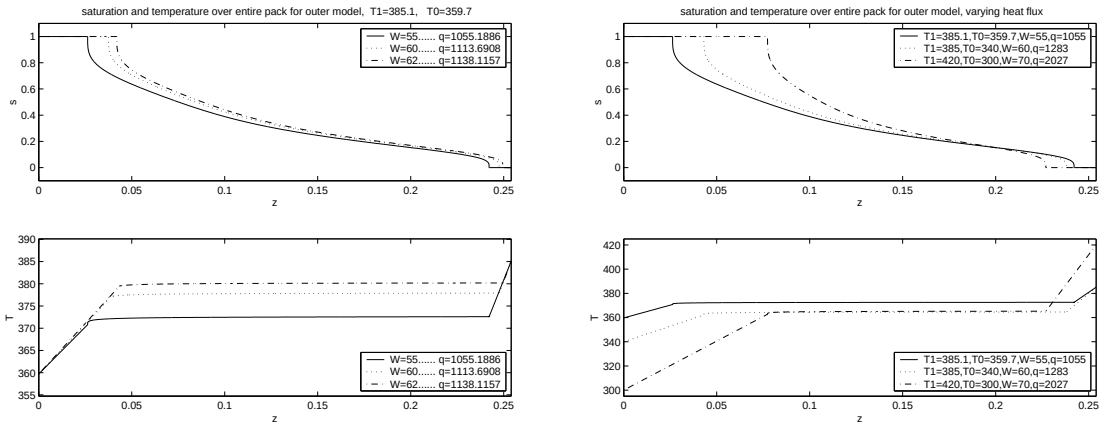

(a) (b)

Figure 6: (a) Profiles for entire pack, with variation in W. (b) Profiles for entire pack, large variation in heat flux.

Algorithm 2

- Input T_1, T_0, W.
- Initialize q, T_{bot}.
- Repeat
  - Compute $\hat{C}$ as in (5.5).
  - Solve the full coupled problem (3.7), (3.8).
  - Hence obtain $s(z)$, $T(z)$, L and T_{top}.
  - (5.2) gives $X = \frac{W-(D-L)\rho_v-\int_0^L(s\rho_l+(1-s)\rho_v)\,dz}{\rho_l-\rho_v}$.
  - $\hat{T}_{dim} = \frac{q(X*lengthscale)}{\hat{K}_l} + T_0$.
  - $\hat{T}_{bot} = \hat{T}_{dim}/T_{ref}$.
  - $q_{top} = \frac{\hat{k}_v(T_1-T_{top}*T_{ref})}{(D-L-X)*lengthscale}$.
  - $g_1(q, T_{bot}) = (q - q_{top})/1000$.
  - $g_2(q, T_{bot}) = T_{bot} - \hat{T}_{bot}$.
  - $\mathcal{G}\begin{pmatrix} q \\ T_{bot} \end{pmatrix} = \begin{pmatrix} g_1(q, T_{bot}) \\ g_2(q, T_{bot}) \end{pmatrix}$.
  - Adjust q and T_{bot} if necessary.
- Until $\|\mathcal{G}\| < tol$.

Here, we define the function g_1 so that it is of order one for the typical values of q under consideration. The tolerance *tol* is a tolerance on the L_2 norm of the error vector $\mathcal{G}$. We implement Algorithm 2 by again employing a Newton method. A good initial guess is required for the Newton method implementation of Algorithm 2, and we take the values we obtain from solving the outer inverse problem. For good initial values of q and T_{bot}, our code converges, again usually in less than 10 iterations. Further, the heat flux q and the temperature T_{bot} converge to values close to those obtained from the outer formulation.

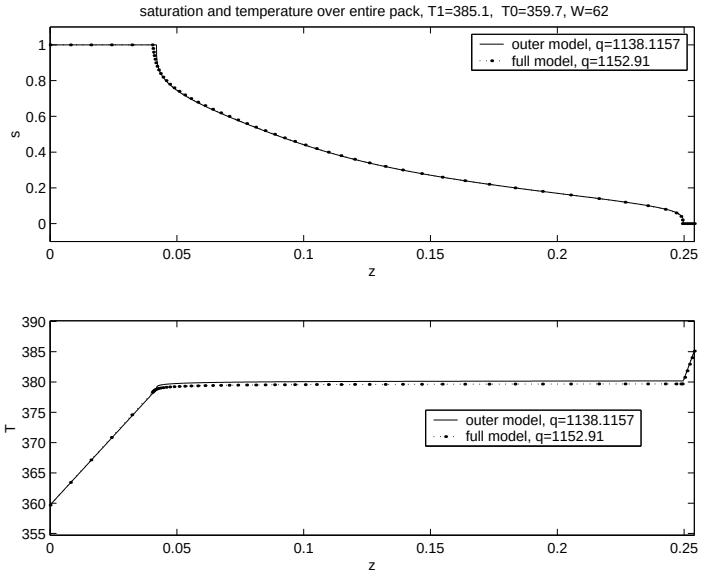

Figure 7: Profiles for entire pack, for outer and full formulations.

In Figure 7, we present the saturation and temperature profiles over the entire pack for both the outer and full models, given the same control parameters. The agreement is excellent. The computed heat flux for the two different formulations agrees to within 2% in all cases we have tried. The values of mean temperature across the two-phase zone for the full and outer models agree to within 1% in all cases computed.

We remark that the simplified outer formulation derived from a boundary layer argument not only approximates the two-phase zone results for the full model with close agreement, but also the results over the entire porous layer for the full model. Despite the extra singularity which we introduce into the problem by accepting the outer model, we have a much simpler problem to solve. The computational expense in solving the outer problem is less than that for the full problem, in both the solution of the differential equations, and in the calculations for the inverse problem.

6 Conclusions

A new formulation for one-dimensional, steady-state heat and mass transfer in a porous medium with phase change has been presented. We have extended the work of Udell [3] to allow for variations in temperature throughout the two-phase zone of a three zone system.

The analysis reveals a singularity in the saturation profile at the upper boundary of the two-phase system, consistent with an evaporation front at this boundary. However, the saturation is found to be analytic at the lower boundary, and so the condensation does not necessarily take place at a front as previously assumed (cf. [3]), but rather we allow for phase-change within the two-phase zone.

We have identified a boundary layer near the lower boundary of the two-phase zone, in which phase change effects and heat diffusion are important, and an outer region, where these effects are negligible. The outer equations are consistent with Udell's model [3], and approximate the full model in the limit of a large vapour pressure gradient.

For realistic parameter values for the entire three-zone system, we have developed an iterative method that finds both the length and the position of the two-phase zone under steady-state conditions. This problem has not been considered previously. Heat transfer is considered separately for the liquid, the two-phase, and the vapour zones, and then the solutions for the three distinct zones are coupled together through the continuity of the temperature. The iterative inverse problem has been solved for both the full and the outer formulations, and close agreement has been obtained.

Since the outer model is identified as a good approximation of the full model for both the two-phase zone calculations and those for the entire system, it is proposed that we accept the outer model in preference to the full model, as it is seen to be significantly less expensive computationally. Further work should include an asymptotic analysis, with the aim of replacing the full model with the outer model subject to an interface condition at the lower boundary. Once this reduced system is derived, it should be possible to use standard computational capturing techniques to compute the boundaries of two-phase zones in more physically realistic two-dimensional models of a porous fuel cell electrode.

Acknowledgements

This work was supported by MITACS in collaboration with our industrial partner Ballard Power Systems. The financial support of MITACS in the way of a student fellowship for L. Bridge is gratefully acknowledged. We also acknowledge valuable discussions with Keith Promislow and Brian Seymour of our local MITACS group.

References

[1] S. Whitaker, Simultaneous heat, mass and momentum transfer in porous media: a theory of drying, *Adv. Heat Trans.,* 13, (1977), pp. 119-203.

[2] R. Bradean, K. Promislow, B. Wetton, Heat and mass transfer in porous fuel cell electrodes. In: G. de Vahl Davis and E. Leonardi (ed.), *Proceedings of the International Symposium on Advances in Computational Heat Transfer*, Vol. 2. Palm Cove (Queensland, Australia), May 2001, pp. 969-976. Publisher: Begell House Inc., New York, USA.

[3] K. S. Udell, Heat transfer in porous media heated from above with evaporation, condensation, and capillary effects, *Journ. Heat Trans.,* 105, (1983), pp. 485-492.

[4] K. E. Torrance, Phase-Change Heat Transfer in Porous Media, *Heat Transfer,* 1, (1986), pp. 181-188.

[5] F. A. Williams, *Combustion Theory: Second Edition*, Benjamin/Cummings Publishing Company, Menlo Park, California, (1985), 680pp.

[6] A. K. Kapila, B. J. Matkowsky, Reactive-diffuse systems with arrhenius kinetics: multiple solutions, ignition and extinction, *SIAM J. Appl. Math.,* 36, (1979), pp. 373-389.

[7] A. K. Kapila, *Asymptotic Treatment of Chemically Reacting Systems*, Applicable Mathematics Series, Pitman (Advanced Publishing Program), Boston MA, (1983), 119pp.

[8] P. Baggio, C. Bonacina, B. A. Schrefler, Some considerations on modeling heat and mass transfer in porous media, *Transp. Porous Media,* 28, (1997), pp. 233-251.

[9] M. M. Abbott and H. C. Van Ness. *Theory and Problems of Thermodynamics* (2nd edition), McGraw-Hill, New York, (1989), 362pp.

[10] M. C. Leverett, Capillary behaviour in porous solids, *AIME Transac.,* 142, (1941), pp. 152-169.

[11] I. Fatt, W. A. Klikoff, Effect of fractional wettability on multiphase flow through porous media, AIME technical note #2043. *AIME Transactions*, 216, (1959), pp. 246.

[12] L. Bridge, *Condensation in a Porous Medium*, M. Sc thesis, Dept. of Mathematics and the Institute of Applied Mathematics, University of British Columbia, Vancouver, Canada, (2001), 51pp.